

VIOLATION OF THE VOGT-RUSSELL THEOREM FOR HOMOGENEOUS NONDEGENERATE STARS

RICHARD STOTHERS

Institute for Space Studies, Goddard Space Flight Center, NASA

Received 1974 April 29; revised 1974 June 25

ABSTRACT

A systematic study is made of the number and types of solutions of the equilibrium equations of stellar structure, in the case of homogeneous stars of Population I over the mass range 2–1000 M_{\odot} , with four different opacity representations. A variant of the usual “fitting” method permits the simultaneous investigation of convergence and tendency toward multiplicity of the solutions. Quadratic interpolation and extrapolation of Carson’s new opacity tables produces a very large opacity at low temperatures that greatly affects the loose outer layers of massive stars, while leaving the cores practically unaffected. As a result, over a small mass range, well above 100 M_{\odot} , triple solutions exist, always near an effective temperature of $\log T_e \approx 4.73$. In such a situation, a “cool” sequence of low masses overlaps a “hot” sequence of high masses, with a short “middle” sequence of intermediate masses connecting them. Multiplicity is found to be favored by a high helium abundance, a high metals abundance, and fast uniform rotation. Secular stability of the models is discussed. The close resemblance between the kinds of multiplicity found in homogeneous stars and in composite stars is pointed out. A simple classification of the known exceptions to the Vogt-Russell theorem on the uniqueness of stellar structure is given.

Subject headings: instabilities — interiors, stellar — massive stars — opacities — rotation, stellar

I. INTRODUCTION

The Vogt-Russell theorem (Vogt 1926; Russell 1927) for a spherical star in hydrostatic and thermal equilibrium can be succinctly stated as follows (Chandrasekhar 1939): “If the pressure, P , the opacity, κ , and the rate of generation of energy, ϵ , are functions of the local values of ρ , T , and the chemical composition only, then the structure of a star is uniquely determined by the mass and the chemical composition.” Strictly speaking, the second adiabatic exponent, Γ_2 , should be mentioned in addition to the pressure, in order to make explicit allowance for the possibility of convective (adiabatic) layers in the star. The “proof” of the theorem is essentially a plausibility argument built around an inspection of the basic equations and boundary conditions, and has never been made mathematically rigorous. Indeed, it cannot (see, e.g., Russell 1927, 1931; Odgers 1957; Chiu 1968; Kähler 1972), and exceptions to both the existence and the uniqueness of the solution of the basic equations are known.

The principal exception to the existence part of the theorem is the occurrence of a maximum mass for cold degenerate (in the sense of fermion degeneracy) stellar models, as was first recognized by Anderson (1929) and, more precisely, by Chandrasekhar (1931). Four exceptions to the statement of uniqueness are known. First, a hot nondegenerate model burning nuclear fuel (a “main-sequence” star) and a cold degenerate model (a white dwarf) can be constructed over a limited range of stellar masses, as was first recognized, in basic principle, by Milne (1930). Second, two (or more) models for a hot partially degenerate star of low mass that is burning nuclear fuel are also calculable, as was first shown by Cox and Salpeter (1964) for helium stars. These two violations of the Vogt-Russell theo-

rem, however, are really only one (see, e.g., Paczynski and Kozłowski 1972). In fact, Milne (1930) and Russell (1931) had already foreseen the possibility of this type of exception to the theorem, although Milne was thinking more in terms of a possible *continuum* of models, which apparently does not exist. The third exception to the theorem is the existence of two models for a nondegenerate star composed of an isothermal core and an envelope of lighter material, separated by a nuclear-burning shell, as was first shown by Gabriel and Ledoux (1967) for intermediate-mass stars with helium cores and hydrogen-rich envelopes. When the core is degenerate, additional models also exist (Kozłowski and Paczynski 1973). The fourth exception is similar to the third (for nondegenerate stars) except that the core need not be isothermal, as was first recognized, in essence, by Stothers and Chin (1968) and, independently, by Paczynski (1970) in the case of massive stars burning helium in the core. The roles of the Chandrasekhar (1931) mass limit for degenerate stars and of the Schönberg-Chandrasekhar (1942) mass limit for an isothermal core are crucial in understanding the divisions between the various exceptions to the theorem for real stars (see, e.g., Paczynski 1972; Kozłowski and Paczynski 1973).

In the present paper we shall show that, for a particular choice of opacity, at least three models for a homogeneous star of high mass are possible. Electron degeneracy, however, is unimportant in this case, and the character of the multiple solutions resembles closely that found in the fourth exception to the Vogt-Russell theorem mentioned above. Specifically, the core structures (and hence the luminosities) of the three models are virtually identical, and only the envelope structures differ.

II. METHOD OF SOLUTION

Models of homogeneous stars of high mass have been constructed with the same input physics and assumptions as were used by Stothers and Simon (1970). However, as a source of opacity, we have used not only the Cox-Stewart "hydrogenic" opacities, as represented by the interpolation formula in the cited paper, but also pure Thomson scattering by free electrons and Carson's (1974) new "Thomas-Fermi" opacities, in the form of tables giving $\log \kappa$ as a function of $\log T$ and $\log \rho$. Both linear and quadratic interpolation in the tables have been employed. Convection, wherever it occurs in the stellar models, has been treated as being adiabatic.

The manner of construction of the models is important here because it has led to the accidental discovery of the multiple solutions. The "fitting" method of solving the basic equations of stellar structure in *nondimensional* form, as described elsewhere (Stothers 1963), is adopted, except that the radiative-envelope parameter C is replaced by $C\kappa/[0.19(1 + X)]$ in order to allow for a full opacity; and *two* eigenvalues for the envelope solutions are now necessary and are here taken to be $\log L$ and $\log T_e$, while the (single) eigenvalue for the convective-core solution is, as before, the central ratio of gas pressure to total pressure, β_c . Fitting of the envelope and core solutions is accomplished at the convective-core boundary with the help of the usual homology invariants; an accuracy of four significant figures is required for a satisfactory fit. The crucial difference in our present approach is that $\log T_e$ is first *specified* (by guessing it) and the value of $\log L$ which gives a fitted solution with respect to the homology invariants is solved for. This yields a "trial" model. Integration of the nuclear-energy generation rate, in nondimensional variables, over the whole convective core provides a relation between R and L , which, between them, produces a *predicted* estimate for $\log T_e$. We shall denote the difference between the logarithms of the two effective temperatures, in the sense of "predicted" minus "specified," as $\delta \log T_e$. Then the rate at which $\delta \log T_e$ changes with the specified value of $\log T_e$ indicates the rate at which the solution is converging to a "final" model.

Difficulties in convergence were encountered at several masses when Carson's opacities were employed. This prompted a systematic search of the $(\log T_e, \delta \log T_e)$ -plane at these masses, with the eventual discovery of both divergent solutions and multiple final models.

III. CONVERGENT AND DIVERGENT SOLUTIONS

The approach of the trial solutions to a definitive solution will be described first for the simplest case where only one final model exists. For simplicity, we assume that the locus of trial solutions on the $(\log T_e, \delta \log T_e)$ -plane is nearly a straight line in the vicinity of the definitive solution. We define $D = d\delta \log T_e / d\log T_e$ at the point $\delta \log T_e = 0$. Then the behavior

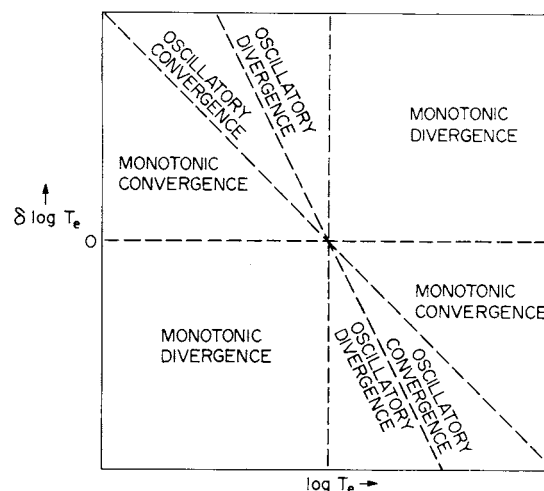


FIG. 1.—Domains of convergent and divergent trial solutions in a plot of specified effective temperature against the "predicted" correction to the specified effective temperature. The horizontal and vertical scales are taken to be equal. The locus of trial solutions may be thought of as a straight line running through the center.

of the trial solutions near this point can be characterized as follows:

- $-\infty < D < -2$: oscillatory divergence;
- $-2 < D < -1$: oscillatory convergence;
- $-1 < D < 0$: monotonic convergence;
- $0 < D < +\infty$: monotonic divergence.

The situation is illustrated in figure 1, where the locus of trial solutions is supposed to be a straight line through the center of the figure. Notice that the convergent trial solutions are confined to the narrow domain: $-2 < D < 0$ (immediate convergence occurs if $D = -1$). This means that, if the specified value of $\log T_e$ is too high (too low), the correction to it, $\delta \log T_e$, is sufficiently negative (positive) to ensure convergence by a process of repeated substitutions of $\log T_e$. In practice, except in the neighborhood of multiple final models, the locus of trial solutions is in fact found to be very nearly a straight line, so that D is normally a well-defined quantity.

Our most exhaustive study treats the mass range $2\text{--}1000 M_\odot$ with a (hydrogen, metals) content of $(X, Z) = (0.49, 0.02)$. Ignoring for the moment the subrange of masses where multiple final models occur, we find that D becomes progressively more negative with increasing stellar mass and also with an increasingly stronger opacity source. This is exemplified by the following results: (1) for pure Thomson scattering by free electrons, $D = -1$ at all masses; (2) for the Cox-Stewart opacities, D approaches -1 asymptotically with increasing mass; (3) for the Carson opacities with *linear* interpolation in the opacity tables, D attains -1 at $\sim 500 M_\odot$ and -2 at $\sim 1000 M_\odot$; and (4) for the Carson opacities with *quadratic* interpolation in the opacity tables, D attains -1 at $\sim 180 M_\odot$ and -2 at

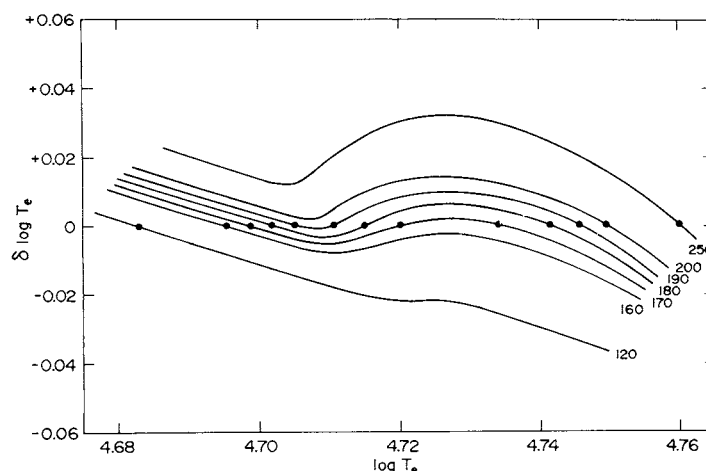


FIG. 2.—Curves of trial solutions for various stellar masses (given in solar units) in a plot of specified effective temperature against the “predicted” correction to the specified effective temperature. Dots indicate definitive solutions. The models have been constructed with $(X, Z) = (0.49, 0.02)$, no rotation, and quadratic interpolation in Carson’s opacity tables.

$\sim 250 M_{\odot}$. Thus, for sufficiently high masses, the use of Carson’s opacity tables renders the trial solutions oscillatory divergent, even though final models do exist.

IV. MULTIPLE SOLUTIONS

The locus of trial solutions on the $(\log T_e, \delta \log T_e)$ -plane for any model built with the Cox-Stewart opacities is very nearly linear even at large distances from the definitive solution. The greater magnitude and the greater irregularity of the Carson opacities produce a wavier line on this plane when the stellar mass is high. But of vastly greater significance is the development of a distinct “bump” on this line when *quadratic* interpolation is employed in Carson’s tables. For reasons to be discussed in § V, quadratic interpolation yields a larger opacity than does linear interpolation at low temperatures and densities in Carson’s tables. Thus the bump on the locus of trial solutions in the $(\log T_e, \delta \log T_e)$ -plane is the consequence of a very large opacity that occurs in the outer layers of massive stellar models.

a) Effect of Stellar Mass

A specific example of the development of such a bump is given in figure 2 for the composition mixture $(X, Z) = (0.49, 0.02)$. Notice that the bump begins its development below the axis of definitive solutions. As the stellar mass increases, the bump expands both horizontally and vertically. These motions carry it up to and, eventually, past the axis of definitive solutions. However, the bump always remains centered at $\log T_e \approx 4.73$.

Any intersection of the curve of trial solutions with the horizontal axis produces a true solution. At low mass, only one true solution exists because the curve is linear. With an increase of mass, a bump on the curve begins to develop, near $\sim 120 M_{\odot}$. However, the top of the bump does not meet the axis of definitive solutions

until a mass of $166 M_{\odot}$ is attained. At this point a *second* definitive solution suddenly appears. It is a degenerate solution because a further slight increase of mass resolves it into two closely spaced components. These second and third solutions proceed to move away from each other, one of them approaching the first solution. Eventually, the two approaching solutions coalesce as the bump on the curve of trial solutions leaves the axis of definitive solutions. This happens at $195 M_{\odot}$. For higher masses, only one solution exists, because the bump, although continually growing, nowhere intersects the horizontal axis.

If the definitive solutions are plotted in a diagram of mass against effective temperature, a single continuous curve results (see fig. 3). Although only one mass exists at any effective temperature, each mass may have up to three effective temperatures associated with it. Division of the curve into three segments allows one easily to visualize a “cool” sequence extending from very low masses up to $195 M_{\odot}$, a short “middle” sequence connecting the “cool” model at $195 M_{\odot}$ with a “hot” model at $166 M_{\odot}$, and a “hot” sequence extending from $166 M_{\odot}$ up to very high masses. The effective temperature rises with increasing mass except on the “middle” sequence and except at extremely high masses on the “hot” sequence. (A tendency toward a constant effective temperature at very high masses occurs even when a purely electron-scattering opacity is adopted [Stothers 1966].)

Since the luminosity at fixed mass is virtually independent of the effective temperature, a diagram with these two quantities plotted would qualitatively resemble figure 3. The physical reason for this is that the cores of the multiple models are nearly identical, only the envelopes differing. (However, close examination does show a very slight increase of luminosity and central radiation pressure due to the reduction of opacity when the effective temperature is hotter.) The main properties of the models are listed in table 1 for several masses.

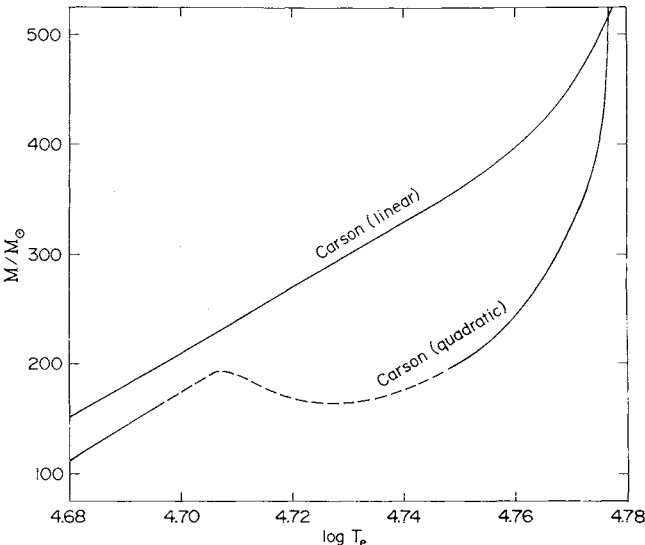


FIG. 3.—Diagram of stellar mass against logarithm of effective temperature, for final stellar models constructed with $(X, Z) = (0.49, 0.02)$, no rotation, and two modes of interpolation in Carson's opacity tables. The dashed portion of the lower line indicates the region of multiple models.

b) Effect of Chemical Composition

Stellar models have also been calculated for the two composition mixtures $(X, Z) = (0.73, 0.02)$ and $(0.71, 0.04)$ in addition to the case just discussed. As before, a bump on the $(\log T_e, \delta \log T_e)$ -plane develops and grows with increasing mass—again around $\log T_e \approx 4.73$. But the stellar mass at which the bump begins is $\sim 270 M_\odot$ and $\sim 300 M_\odot$ for the above two mixtures, respectively. Evidently the effect of mean molecular weight (through the hydrogen and helium abundances primarily) is more important than the effect of opacity (mostly through the metals abundance) in determining the mass at which the bump develops. In the case $(X, Z) = (0.73, 0.02)$ the bump is just starting to develop as its top reaches the axis of definitive solutions. If either X were larger or Z smaller, the bump would begin to develop *above* this axis, and bifurcation of the models would be avoided at all masses in this case.

Characteristics of the models that lie at the bifurcation points are given in table 2 for three chemical compositions.

c) Effect of Uniform Rotation

The basic equations for a uniformly rotating star may be conveniently reduced to the same form as for a spherical star by introducing the simple parameter $\alpha = \frac{2}{3}\Omega^2 r^3/GM(r)$, where Ω is the angular velocity about the rotation axis (Faulkner, Roxburgh, and Strittmatter 1968). The Vogt-Russell theorem ought therefore to cover the case of a star in uniform rotation if Ω is specified. Or, equivalently, the surface parameter $\lambda = \frac{2}{3}\Omega^2 R^3/GM$ may be specified.

Adopting the reduced equations, we investigate the effect of an increase of λ on the structure of the stellar models for $180 M_\odot$ with $(X, Z) = (0.49, 0.02)$. As is well known, the core structure (and hence the luminosity) remains almost unaltered by uniform rotation,

TABLE 1
NONROTATING STELLAR MODELS CONSTRUCTED WITH $(X, Z) = (0.49, 0.02)$
AND QUADRATIC INTERPOLATION IN CARSON'S OPACITY TABLES

M/M_\odot	$\log T_e$	$\log L/L_\odot$	$\log R/R_\odot$	$\log T_c$	$\log \rho_c$	β_c	$\rho_c/\langle\rho\rangle$
120.....	4.682	6.374	1.349	7.655	0.188	0.427	102
160.....	4.695	6.553	1.412	7.663	0.131	0.380	103
170.....	4.698	6.589	1.424	7.665	0.118	0.371	103
	4.720	6.589	1.381	7.665	0.118	0.371	76
	4.735	6.589	1.352	7.665	0.118	0.371	62
180.....	4.702	6.623	1.434	7.667	0.107	0.362	102
	4.715	6.623	1.409	7.667	0.107	0.362	85
	4.741	6.623	1.355	7.667	0.107	0.362	59
190.....	4.705	6.655	1.443	7.668	0.096	0.354	100
	4.711	6.655	1.433	7.668	0.096	0.354	93
	4.746	6.655	1.362	7.668	0.096	0.354	57
200.....	4.749	6.685	1.370	7.670	0.086	0.346	56
250.....	4.761	6.810	1.409	7.675	0.044	0.316	53

TABLE 2
NONROTATING STELLAR MODELS BASED ON QUADRATIC INTERPOLATION IN CARSON'S
OPACITY TABLES AND LOCATED AT THE BIFURCATION POINTS

X	Z	M/M_{\odot}	$\log T_e$	$\log L/L_{\odot}$	β_c	$\rho_c/\langle\rho\rangle$
0.49.....	0.02	166	4.697	6.575	0.376	103
			4.727	6.575	0.376	66
		195	4.707	6.670	0.350	97
0.73.....	0.02	292	4.748	6.670	0.350	56
			4.717	6.782	0.350	64
		295	4.728	6.782	0.350	55
			4.718	6.788	0.348	64
0.71.....	0.04	480	4.729	6.788	0.348	55
			4.702	7.062	0.278	91
		585	4.736	7.063	0.278	56
			4.713	7.167	0.255	84
			4.750	7.168	0.255	51

while the envelope expands, thereby reducing the effective temperature (in the mean sphere approximation). We find, in figure 4, that the bump on the line of trial solutions in the $(\log T_e, \delta \log T_e)$ -plane becomes depressed below the axis of definitive solutions and its height decreases (both linearly with increasing λ), although the top of the bump remains centered at $\log T_e = 4.727$ even for critical rotation at the star's equator ($\lambda = 0.30$). The bump leaves the axis of definitive solutions when $\lambda = 0.07$. However, the "cool" model still exists, with its temperature dropping linearly with increasing λ until it attains $\log T_e = 4.669$ at critical rotation. By comparison with figure 2, we see that uniform rotation produces the same effect on the multiplicity of solutions as does a reduction of the stellar mass. Consequently, although uniform rotation lifts the mathematical degeneracy found in § IVa for a newly developed solution at a bifurcation point, it does not completely remove the incidence of degeneracy from the mass spectrum but puts it somewhere else (i.e., at higher masses).

One further effect, not seen for the zero-rotation

models, is the development of a *second* bump on the $(\log T_e, \delta \log T_e)$ -plane above the axis of definitive solutions. This new bump develops around $\log T_e = 4.635$ in figure 4, but its location and small size clearly indicate that it plays no role in adding further final models for the adopted chemical composition. Its interest lies in the possibility, for some other chemical composition and mass, of the existence of *five* final models, if the rotation is fast enough.

V. PHYSICAL INTERPRETATION

Carson's (1974) new opacities are based on the hot "Thomas-Fermi" atomic model for all elements heavier than hydrogen and helium. Unlike the available "hydrogenic" opacities, such as those of Cox and Stewart (1965), they do not slope off smoothly to the Thomson electron-scattering limit as the density is decreased or as the temperature is increased. Rather, a large "bump," due to the last stages of ionization of the CNO group of elements, shows up in the opacity curves at very low densities, particularly for temperatures

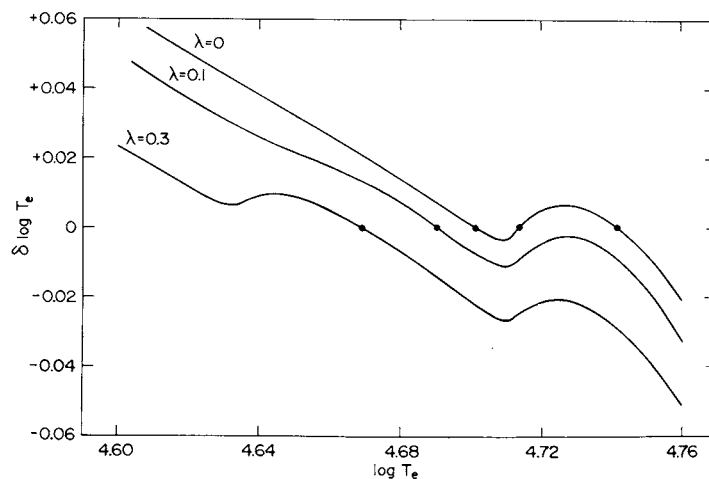


FIG. 4.—Curves of trial solutions for uniformly rotating models of $180 M_{\odot}$ in a plot of specified effective temperature against the "predicted" correction to the specified effective temperature. Dots indicate definitive solutions. The models have been constructed with $(X, Z) = (0.49, 0.02)$ and quadratic interpolation in Carson's opacity tables. The curves are labeled with the rotation parameter λ .

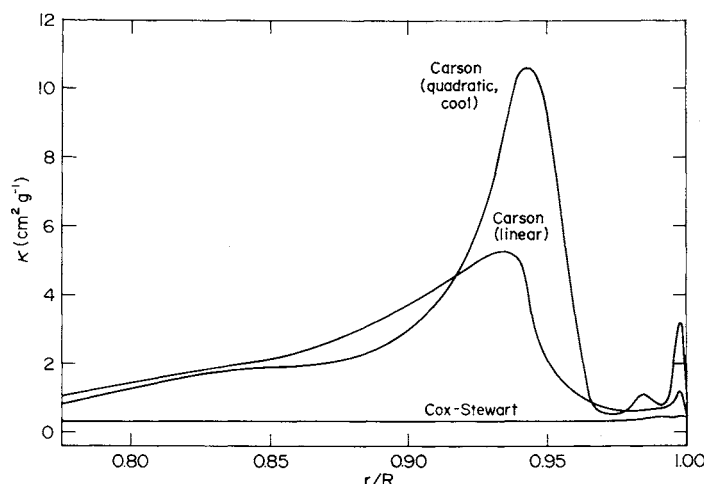


FIG. 5.—The run of opacity with radius fraction for nonrotating stellar models of $180 M_{\odot}$ with $(X, Z) = (0.49, 0.02)$ and three different opacity representations. The mode of interpolation in the opacity tables is indicated for Carson's opacities.

between $\log T = 5.5$ and 6.2 , although much substructure in the opacity curves is also evident. Carson's opacity tables extend to a sufficiently low density that the initial rise of the bump is well covered; however, the second derivative in the curvature of the bump is not determined. Therefore, quadratic extrapolation of his tables to very low densities produces a much larger opacity than does linear extrapolation, in the neighborhood of the bump. In this way, other, smaller irregularities also tend to become exaggerated (for example, the bump due to helium ionization at a lower temperature). In general, we have found it necessary to extrapolate Carson's tables for temperatures below $\log T = 5.8$ in stars more massive than $\sim 30 M_{\odot}$, where the densities are very low. From the heuristic point of view of the present paper, it makes no difference whether the large opacities (however they are obtained) are correct or not. Nevertheless, computation of a few additional opacity points in order to

extend Carson's tables gives values which are approximated better by linear than by quadratic extrapolation from the original tables.

In figure 5, the run of opacity with radius fraction is shown for three stellar models with mass $180 M_{\odot}$ and $(X, Z) = (0.49, 0.02)$. The large bump due to CNO ionization and the smaller bump (near the surface) due to helium ionization are exaggerated when quadratic extrapolation is used in Carson's opacity tables. But wherever interpolation in the tables is used, linear interpolation is found to give the larger opacity. Insofar as multiplicity of the stellar models is concerned, the size of the large bump appears to be the main contributing factor, since the location of this bump is about the same in the two models shown, which are otherwise very similar. Notice that the third model, constructed with Cox-Stewart opacities, has a run of opacity that is everywhere very nearly equal to the Thomson electron-scattering limit.

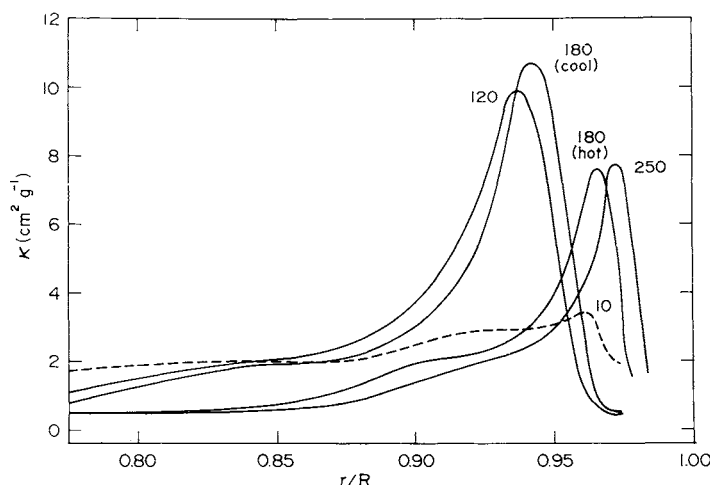


FIG. 6.—The run of opacity with radius fraction for nonrotating stellar models of different masses (given in solar units) constructed with $(X, Z) = (0.49, 0.02)$ and quadratic interpolation in Carson's opacity tables.

In addition to the size of the large opacity bump, the radius position of the bump is also important, as may be seen in figure 6 for stellar models of different masses constructed with quadratic interpolation in Carson's opacity tables. Three features of this figure deserve to be pointed out. First, the opacity bump becomes larger with increasing stellar mass. This produces a large shift in the mass distribution within the envelope, as we shall show below. Actually, the average level of opacity is greater at $10 M_{\odot}$ than at much higher masses, but the run of opacity through the envelope at $10 M_{\odot}$ is very nearly uniform (like Thomson scattering!). Second, the width of the opacity bump shrinks with increasing stellar mass; on the one hand, this shrinkage differentiates the bump more clearly from the background, but, on the other hand, it limits the influence of the bump if too narrow a portion of the star is involved. Third, the radius fraction of the maximum of the bump diminishes with increasing mass up to $\sim 60 M_{\odot}$, but above $\sim 60 M_{\odot}$, the maximum of the bump moves back toward the stellar surface; the reason is that the bump maximum always occurs near $\log T = 5.6$, which, for very high masses, is reached sufficiently close to the surface that a temperature difference here is nearly proportional to a difference in radius fraction. And the models of higher mass have higher surface temperatures. In this connection, it is worth remarking that, for multiple models of the same mass, the "hot" model has a denser envelope than does the "cool" model and therefore the opacities in the outer layers of the "hot" model are smaller. The effects of surface temperature and of envelope density are both demonstrated very clearly in figure 6 for the two models of $180 M_{\odot}$.

We conclude that an opacity which increases rapidly with increasing stellar radius fraction, in such a way that it becomes appreciable at moderate depths below

the surface, is potentially very effective in influencing the structure of a diffuse envelope. Presumably, a modified form of Kramers opacity could be equally as effective as Carson's opacities. It should be emphasized that the effect of the opacity's actual magnitude is only indirect, because, at high masses, the zone with the large opacity is convective (treated here as adiabatic). This zone, in the "cool" models of highest mass, extends down from the atmosphere to a depth of $r/R \approx 0.65$.

Recourse is now made to the (U, V) -plane in order to study the direct effect of the opacity on the envelope structure. First, we consider the case of $180 M_{\odot}$ with the four adopted opacity representations (fig. 7). The minor increase of the Cox-Stewart opacities over the constant Thomson electron-scattering opacity, especially near the stellar surface, increases slightly the central condensation of the envelope, as the reduction in U indicates. Adoption of Carson's large opacities, however, increases the central condensation very markedly, to the point where the envelope and core become quite distinct from each other. The stellar structure thus resembles a giant configuration, whose (U, V) -curve is quite similar to the present one (e.g., Schwarzschild 1958). In the present case, the "base" of the envelope occurs at $M(r)/M = 0.999$ and $r/R = 0.65$, where V has a local minimum, while the convective core boundary occurs at $M(r)/M = 0.926$ and $r/R = 0.39$. Examination of the (U, V) -curves gives no obvious indication why multiple solutions should occur when quadratic interpolation in Carson's opacity tables is used and not when linear interpolation is used. However, figure 5 confirms that very local conditions, affecting only the outermost layers of the star, are sufficient to produce multiplicity.

In figure 8, (U, V) -curves are shown for stellar models of different masses constructed with quadratic

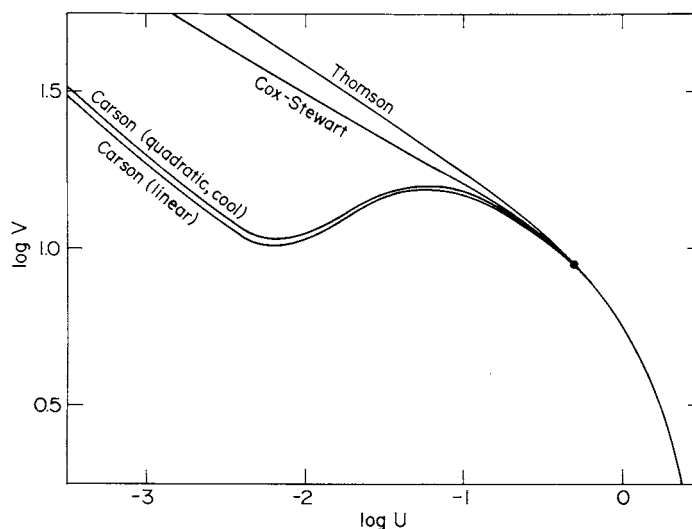


FIG. 7.— (U, V) plane for nonrotating stellar models of $180 M_{\odot}$ with $(X, Z) = (0.49, 0.02)$ and four different opacity representations. The mode of interpolation in the opacity tables is indicated for Carson's opacities. The dot denotes the convective core boundary.

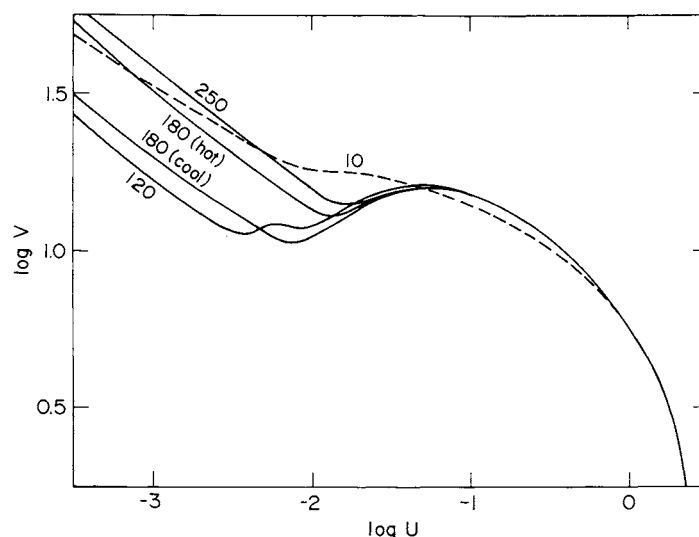


FIG. 8.—(U , V) plane for nonrotating stellar models of different masses (given in solar units) constructed with $(X, Z) = (0.49, 0.02)$ and quadratic interpolation in Carson's opacity tables.

interpolation in Carson's opacity tables. The smallest local minimum of V reflects the highest central condensation of the stellar envelope, and is found to occur precisely in the mass range where multiple solutions exist. This result accords with our intuitive expectation that multiplicity is more likely to occur in more highly differentiated structures. However, unlike the cases already discovered in which a chemical inhomogeneity (i.e., a change in mean molecular weight) produces most of the differentiation in structure, the present instance of multiplicity arises solely from the very large opacity in the outermost layers. Probably the fact that the structural differentiation is not as severe in the present models as in a supergiant is the reason why the present multiple models lie clustered so close together in the $(\log L, \log T_e)$ -diagram.

VI. SECULAR STABILITY OF THE MODELS

Secular (thermal) stability of the models has not been formally tested. However, it is probable that divergence of the trial solutions in the $(\log T_e, \delta \log T_e)$ -plane indicates secular instability. The reason for suspecting this is that $\delta \log T_e$ is, in effect, a measure of the difference between the radiative luminosity emitted by the surface of the star and the nuclear luminosity generated by the core (see § II). Provided that $\delta \log T_e$ is sufficiently small in absolute value, it indicates the correction needed to bring a slightly perturbed model (which is very close to being in hydrostatic equilibrium) back into thermal equilibrium. Jeans (1929) developed a similar diagrammatic approach to the general problem of secular stability, with a formal justification provided by a study of the linearized equations of stellar structure.

On this basis, we suggest that stellar models of sufficiently high mass constructed with Carson's opacities may be secularly unstable, in the sense of overstability, because the trial solutions above a certain

mass are oscillatory divergent. The only definite case of oscillatory secular instability discovered so far is that occurring in the helium-burning shell of an evolved star of low mass (Härm and Schwarzschild 1972). We suggest further, that stellar models on the "middle-temperature" sequence, which exists when quadratic interpolation is used in Carson's opacity tables, may be secularly unstable in the ordinary sense, because the trial solutions for them are always monotonic divergent. Depending on the direction of the initial perturbation, these unstable models would be expected to move either to the "hot" or to the "cool" sequence, on a thermal (Helmholtz-Kelvin) time scale. Interestingly, the "middle-temperature" models for non-degenerate composite configurations (Lauterborn, Refsdal, and Roth 1971; Paczynski 1972) and for low-mass partially degenerate configurations (Gabriel and Noels-Grötsch 1968; Paczynski 1972) may also be secularly unstable.

Support for the present method of inferring secular instability (but, possibly, some doubt about the occurrence of the instability as overstability) is indicated by the following test case. Stars evolving off the zero-age main sequence are well known to be secularly stable, and only to become unstable against a slow overall contraction near the end of core hydrogen burning. At high mass, the contraction begins when the central hydrogen abundance drops to about 0.03. We have here evolved two sequences of static models for $60 M_\odot$ to an arbitrarily small value of central hydrogen abundance. The Cox-Stewart and Carson opacities were adopted. The trial solutions in both cases remained monotonic convergent until $X_c \approx 0.03$; thereupon they became oscillatory divergent.

VII. CONCLUSION

A study has been made of the number and types of solutions occurring for the equilibrium equations of

stellar structure, in the case of homogeneous stars of Population I over the mass range $2\text{--}1000 M_{\odot}$, with the following opacity representations: Thomson electron-scattering opacity, Cox-Stewart "hydrogenic" opacities, and Carson "Thomas-Fermi" opacities. A variant of the usual "fitting" method of solving the basic equations has allowed us to construct a one-parameter family of trial models for each mass and chemical composition. The free parameter, $\log T_e$, and its "correction," $\delta \log T_e$, when plotted against each other, normally form a straight line, whose slope at $\delta \log T_e = 0$ (the final model) indicates convergence or divergence of the solution.

All the models have monotonic convergent solutions except for the models of very high mass constructed with Carson's opacities, whose solutions become oscillatory convergent and, eventually, oscillatory divergent with increasing mass. The use of quadratic interpolation in Carson's opacity tables produces a very large opacity at low temperatures, which ultimately causes a bump to develop on the line of trial solutions in the $(\log T_e, \delta \log T_e)$ -plane. *This bump indicates the tendency toward a multiplicity of final solutions.* It grows with increasing mass and produces two additional final models when it crosses the axis $\delta \log T_e = 0$. However, in a diagram of mass (or luminosity) against effective temperature, all the final models describe a *single continuous curve*, just as Russell (1927) had originally conjectured when thinking about possible exceptions to his theorem. Three sequences of models are represented by segments of this curve, viz., a "cool" sequence at low to intermediate masses, a "middle" sequence at intermediate masses, and a "hot" sequence at intermediate to high masses. In the language of Poincaré a linear series of models exists, having three branches and two bifurcation points, which also happen here to be turning points.

Triple models in the present work occur only over a very small range of masses, well above $100 M_{\odot}$ for a typical Population I chemical composition, and always near $\log T_e = 4.71 \pm 0.01$ for the "cool" models and $\log T_e = 4.74 \pm 0.01$ and $\rho_c \langle \rho \rangle = 60 \pm 5$ for the "hot" models. The whole mass range is shifted upward for a lighter mean molecular weight or for a faster uniform rotation. However, a lighter mean molecular weight (i.e., a higher hydrogen abundance) or a smaller opacity (i.e., a lower metals abundance) disfavors the occurrence of multiplicity. Models on the "middle"

sequence of stars are probably secularly unstable; models of very high mass on the "hot" sequence are probably also secularly unstable (possibly in the sense of overstability).

The multiplicity of solutions found here for homogeneous stars bears a strong resemblance to that discovered earlier for composite stars (Stothers and Chin 1968; see also Paczynski 1970, 1972; Lauterborn *et al.* 1971; Lauterborn 1973). First of all, the range of multiplicity of the solutions increases with stellar mass, although triple solutions are the most commonly found. Second, the core structures of a multiplet are virtually identical, while only the envelope structures differ. Third, the state of the gas is nondegenerate throughout the models. Fourth, a nonconstant opacity source (with high values of opacity in the outermost layers) and a large central condensation of the envelope are the apparent causes of the multiplicity. Fifth, a single characteristic curve is described by the models on a diagram of effective temperature against total mass (for homogeneous models) or core mass (for composite models). Sixth, the range of total stellar masses or of core masses over which multiple models exist is very limited. Seventh, the effective temperatures of the multiple models on the "hot" and "cool" sequences are nearly invariant quantities. Eighth, the "middle-temperature" models are probably secularly unstable.

It is possible to group the known exceptions to the Vogt-Russell theorem into three categories of stars: (1) partially to completely degenerate stars of intermediate to low mass, for which three or more models exist with different core and envelope structures; (2) nondegenerate to partially degenerate stars of intermediate mass, for which two models exist with different isothermal-core structures but similar envelope structures; and (3) nondegenerate stars of high mass, for which three or more models exist with nearly identical core structures but different envelope structures. There is some overlap of these three categories. Perhaps the most remarkable result is that a complex chemical structure is not necessary to produce multiple solutions for a nondegenerate star. A variable opacity, alone, can do this.

Dr. T. Richard Carson very kindly permitted me to use his tables of opacities in advance of their publication.

REFERENCES

- Anderson, W. 1929, *Zs. f. Phys.*, **56**, 851.
 Carson, T. R. 1974, in preparation.
 Chandrasekhar, S. 1931, *M.N.R.A.S.*, **91**, 456.
 ———. 1939, *An Introduction to the Study of Stellar Structure* (Chicago: University of Chicago Press), p. 252.
 Chiu, H.-Y. 1968, *Stellar Physics* (Waltham, Mass.: Blaisdell), p. 421.
 Cox, A. N., and Stewart, J. N. 1965, *Ap. J. Suppl.*, **11**, 22.
 Cox, J. P., and Salpeter, E. E. 1964, *Ap. J.*, **140**, 485.
 Faulkner, J., Roxburgh, I. W., and Strittmatter, P. A. 1968, *Ap. J.*, **151**, 203.
 Gabriel, M., and Ledoux, P. 1967, *Ann. d'Ap.*, **30**, 975.
 Gabriel, M., and Noels-Grötsch, A. 1968, *Ann. d'Ap.*, **31**, 167.
 Härm, R., and Schwarzschild, M. 1972, *Ap. J.*, **172**, 403.
 Jeans, J. H. 1929, *Astronomy and Cosmogony* (Cambridge: Cambridge University Press), pp. 146–150.
 Kähler, H. 1972, *Astr. and Ap.*, **20**, 105.
 Kozłowski, M., and Paczynski, B. 1973, *Acta Astr.*, **23**, 65.
 Lauterborn, D. 1973, *Astr. and Ap.*, **27**, 323.
 Lauterborn, D., Refsdal, S., and Roth, M. L. 1971, *Astr. and Ap.*, **13**, 119.
 Milne, E. A. 1930, *M.N.R.A.S.*, **91**, 4.
 Odgers, G. J. 1957, *Pub. Dom. Ap. Obs. (Victoria)*, **10**, 393.
 Paczynski, B. 1970, *Acta Astr.*, **20**, 195.
 ———. 1972, *ibid.*, **22**, 163.
 Paczynski, B., and Kozłowski, M. 1972, *Acta Astr.*, **22**, 315.

- Russell, H. N. 1927, in *Astronomy*, by H. N. Russell, R. S. Dugan, and J. Q. Stewart (Boston: Ginn & Co.), Vol. 2, pp. 910–911.
- . 1931, *M.N.R.A.S.*, **91**, 951.
- Schönberg, M., and Chandrasekhar, S. 1942, *Ap. J.*, **96**, 161.
- Schwarzschild, M. 1958, *Structure and Evolution of the Stars* (Princeton: Princeton University Press).
- Stothers, R. 1963, *Ap. J.*, **138**, 1074.
- . 1966, *ibid.*, **144**, 959.
- Stothers, R., and Chin, C.-w. 1968, *Ap. J.*, **152**, 225.
- Stothers, R., and Simon, N. R. 1970, *Ap. J.*, **160**, 1019.
- Vogt, H. 1926, *Astr. Nach.*, **226**, 301.

RICHARD STOTHERS: Institute for Space Studies, Goddard Space Flight Center, NASA, 2880 Broadway, New York, NY 10025